S_N2 Reactions as Two-State Problems: Diabatic MO-CI Calculations on Li_3^-, Li_2H^-, Cl_3^-, and $ClCH_3Cl^-$

O. K. Kabbaj,[†] M. B. Lepetit,[‡] J. P. Malrieu,*[,‡] G. Sini,[§] and P. C. Hiberty[§]

Contribution from the Laboratoire de Chimie Théorique, Faculté des Sciences, Rabat, Morocco, Laboratoire de Physique Quantique (U.A. 505 du C.N.R.S.), Université Paul Sabatier, 118, route de Narbonne, 31062 Toulouse Cedex, France, and Laboratoire de Chimie Théorique (U.A. 506), Université de Paris-Sud, 91405 Orsay Cedex, France. *Received November 21, 1990*

Abstract: A diabatic interpretation of S_N2 reactions $A^- + BC \rightarrow AB + C^-$ has been recently proposed by Shaik and Pross, which relates the barrier heights to the electroaffinities of A and BC reactant systems. This model rests on qualitative VB correlation diagrams. The present work proposes a similar diabatic picture of these reactions, based on ab initio MO-CI calculations in extended basis sets. The two lowest adiabatic $^1\Sigma^+$ states are rotated to generate nearly diabatic states, providing nearly diabatic potential surfaces correlating $A^- + BC$ and $AB^- + C$ for one of them, $A + BC^-$ and $AB + C^-$ for the other, and an effective coupling between them. The procedure is applied to two symmetrical reactions (Li_3^- and Cl_3^-) and one nonsymmetrical reaction (Li_2H^-) and may be easily fitted by LEPS-type interpolations, irrespective of the stability of the transition complex. Since the LEPS functions are built from the Morse representation of the asymptotic potential curves of BC, BC^-, AB, and AB^-, improved estimates of the potential surfaces (both diabatic and adiabatic) may be obtained by fitting the asymptotes on experimental values and keeping the interaction constant, as proved on the Cl_3^- problem. For the sake of comparison, some direct valence bond calculations of diabatic and adiabatic surfaces are also performed. The relevance of the S. Shaik's diagrams is discussed. Their availability for more realistic chemical reactions is demonstrated on the $Cl^- + CH_3Cl$ problem.

I. Introduction

A major qualitative success of quantum chemistry in the domain of chemical reactivity was the comprehension of the stereoselectivity of concerted reactions. In that case, symmetry considerations make possible to discriminate between forbidden and allowed reactions.[1] Symmetry-allowed reactions may present potential barriers of various heights or stable reaction complexes, and the MO or configuration correlation diagrams cannot predict the position of the transition state, which has to be calculated numerically. S_N2 reactions belong to the family of symmetry-allowed reactions and provide a good sampling of situations regarding the transition-state position (above or below the reactants energy).

Ten years ago S. Shaik[2] proposed a qualitative model based on valence bond correlation diagrams to rationalize the energy profile of the reaction pathway. For an $A^- + BC \rightarrow AB + C^-$ reaction, Shaik proposed to correlate the entrance channel with the charge-transfer state of the products and vice versa as pictured in Figure 1.

This correlation is intuitively based on the left-right position of the supplementary electron, which is grossly maintained in the VB correlation. A crucial quantity in such a diagram is the energy separation G between the entrance (or product) ground state and the charge-transfer excited state; this quantity is simply the difference between the electroaffinities of A and BC (or AB and C)

$$G = EA(A) - EA(BC)$$

This quantity may vary significantly from one reaction to another. The model[3] of course considers the interaction between the two "states" and assumes that the amplitude B of this interaction at the curve crossing is more or less constant. At this stage, for a symmetrical reaction the barrier is given by

$$E_S = \frac{G}{2} - B$$

which may be either positive (barrier height) or negative (stable intermediate). The model has been sophisticated[4] by considering the curvature of the correlating curves and by saying that their intersection lies at the position fG above the entrance channel. Then

$$E_S = fG - B$$

This model has proved to be efficient to rationalize a lot of experimental informations.

The VB correlation diagram looks like the diabatic transcription of a two-state problem, i.e., the interaction between two diabatic surfaces dissociating in the proper physical asymptotes namely $AB + C^- \rightarrow A + BC^-$ and $AB^- + C \rightarrow A^- + BC$. Nearly diabatic approaches are now practically routine in MO-CI calculations,[5,6] and one may be tempted to use that approach to study quantitatively the relevance of the VB diagrams. The use of MO-CI techniques has the advantage of flexibility (possible use of extended basis sets) and accuracy if the CI is sufficiently large. The present paper performs such MO-CI nearly diabatic calculations on three different systems, two of them being symmetrical $Li_2 + Li^-$ and $Cl_2 + Cl^-$, one being nonsymmetrical ($H^- + Li_2 \rightarrow HLi^- + Li^-$). The geometries are kept colinear, as reasonable for S_N2 reactions especially these three ones for which the transition complex is stable and linear. The procedure is developed in the next section, the results are given in section III, and the adequacy of Shaik and Pross's model in view of our results is discussed in the last section. As shown in section III the diabatic surfaces, which have regular shape, may be fitted easily by LEPS formulas.[7] The coupling between the two diabatic states also has a regular dependence on the nuclear coordinates with maximal amplitude on the intersection line. The relevance of the proposed procedure for more chemically realistic problems has been illustrated on the basic S_N2 reaction, namely the $Cl^- + CH_3Cl$ system.

II. Theoretical Methods

(A) Basis Sets and Adiabatic MO-CI Calculation Technique. The core electrons are treated through nonempirical pseudopo-

[†] Faculté des Sciences.
[‡] Université Paul Sabatier.
[§] Université de Paris-Sud.

(1) Woodward, R. B.; Hoffman, R. *J. Am. Chem. Soc.* **1965**, *87*, 395; **1965**, *87*, 2046. Woodward, R. B.; Hoffmann, R. *The Conservation of Orbital Symmetry*; Verlag Chemie: Academic Press, 1970.
(2) Shaik, S. S. *Nouv. J. Chim.* **1982**, *6*, 159. Shaik, S. S.; Pross, A. *J. Am. Chem. Soc.* **1982**, *104*, 2708.
(3) Shaik, S. S. *J. Am. Chem. Soc.* **1981**, *103*, 3692. Pross, A.; Shaik, S. S. *Acc. Chem. Res.* **1983**, *16*, 363. Pross, A. *Adv. Phys. Org. Chem.* **1985**, *21*, 99.
(4) Shaik, S. S. *Prog. Phys. Org. Chem.* **1985**, *15*, 197.
(5) Spiegelmann, F.; Malrieu, J. P. *J. Phys. B* **1984**, *17*, 1259. Gadea, F. X.; Spiegelmann, F.; Pelissier, M.; Malrieu, J. P. *J. Chem. Phys.* **1986**, *84*, 4872.
(6) Bernardi, F.; Robb, M. A. In *Ab initio Methods in Quantum Chemistry*, Lawley, K. P., Ed.; Wiley: New York, 1987; Vol. 1, p 155.
(7) Eyring, H.; Polanyi, M. *Z. Phys. Chem.* **1931**, *12*, 279. Sato, S. *J. Chem. Phys.* **1955**, *23*, 592. Sato, S. *J. Chem. Phys.* **1965**, *43*, 2465. Kuntz, P. J.; Nemeth, E. M.; Polanyi, J. C.; Rosner, D.; Young, C. E. *J. Chem. Phys.* **1966**, *44*, 1168.

0002-7863/91/1513-5619$02.50/0

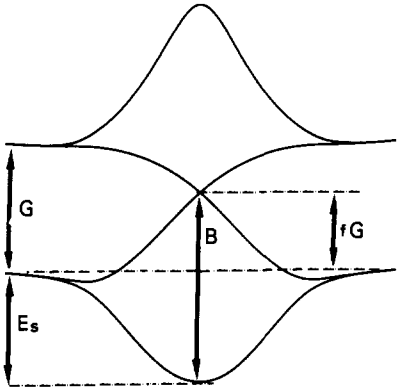

Figure 1. Shaik's VB correlation diagram for S_N2 reactions. Of course B may be smaller than fG, and the reaction will then present a barrier.

tentials proposed by Barthelat and Durand,[8] and the problem thus reduces to valence electrons. The valence basis sets are of the following quality: 3s 2p for H, 3s 2p 1d for Li and Cl; they are given in Table VI.

These basis sets involve rather diffuse AOs in order to obtain reliable atomic electroaffinities. The atomic and molecular adiabatic calculations follow the standard MO-CI approach; the SCF MOs are used in a variational + perturbational CI treatment. For light atoms, diatoms and triatoms involving at most four valence electrons, full CIs were achieved. For Cl_n (n = 1, 3) problems the CI was based on a rational selection, according to the CIPSI algorithm.[9] A zeroth-order wave function is built on the ~200 most important determinants, and it is perturbed to the second order in energy by all the interacting determinants (in number larger than 10^7 for Cl_3^-). This method may be defined as a multireference second-order Moller–Plesset[10] perturbation treatment.

(B) **Nearly Diabatic Approach.** It is known that strictly diabatic wave functions ($\partial\psi/\partial r = 0$) do not exist or are useless. What is desired is some unvariance of the physical content of the wave function, which may be defined from the asymptotic content. With our problem we want to consider the entrance and product ground-state asymptotes (i.e., $A^- + BC$ and $AB + C^-$ for an $A^- + BC \rightarrow AB + C^-$ reaction) as our guidelines for the diabatization.

The basic idea will consist of a rotation of the two lowest singlet $^1\Sigma^+$ adiabatic states, in order to obtain two "diabatic" states, of course electronically coupled, which look like the reference asymptotic states.[11,12] One has then two adiabatic eigenstates of the electronic Hamiltonian ψ and ψ^*

$$H\psi = E\psi \qquad H\psi^* = E^*\psi^*$$

and the two reference asymptotic functions R_1 and R_2

$$R_1 = |a\bar{a}(b\bar{c} + c\bar{b})|/\sqrt{2} \text{ (VB description of } A^- + BC)$$

$$R_2 = |(a\bar{b} + b\bar{a})c\bar{c}|/\sqrt{2} \text{ (VB description of } AB + C^-)$$

where a, b, and c are the concerned valence AOs of the atoms AB and C. For any nuclear conformation, one projects R_1 and R_2 into the subspace defined by ψ and ψ^*

$$|\tilde{R}_1\rangle = |\psi\rangle\langle\psi|R_1\rangle + |\psi^*\rangle\langle\psi^*|R_1\rangle$$

$$|\tilde{R}_2\rangle = |\psi\rangle\langle\psi|R_2\rangle + |\psi^*\rangle\langle\psi^*|R_2\rangle$$

and one symmetrically orthogonalizes these projections through the $S^{-1/2}$ procedure to obtain two orthogonal vectors $|R'_1\rangle$ and $|R'_2\rangle$ which span the same subspace as ψ and ψ^*

$$\{R'_1, R'_2\} = S^{-1/2}\{\tilde{R}_1, \tilde{R}_2\}$$

$$R'_1 = \cos\alpha\psi + \sin\alpha\psi^*$$

$$R'_2 = -\sin\alpha\psi + \cos\alpha\psi^*$$

Notice that the states R'_1 and R'_2 do not interact with the eigenstates of $\mathcal{H}$ besides ψ and ψ^*. The information is now given by the Hamiltonian in its 2 × 2 block spanned by R'_1 and R'_2

$$\langle R'_1|\mathcal{H}|R'_1\rangle = \cos^2\alpha E + \sin^2\alpha E^*$$

will give us the diabatic potential surface related to R_1 and $\langle R'_2|\mathcal{H}|R'_2\rangle$ gives the second diabatic potential surface related to R_2. $\langle R'_1|\mathcal{H}|R'_2\rangle$ represents the electronic coupling between the two diabatic states. It is easy to see that in the entrance channel

$$\langle\psi|R_1\rangle \neq 0 \text{ (and close to 1)}$$

$$\langle\psi^*|R_1\rangle = 0$$

$$\langle\psi|R_2\rangle = 0$$

$$\langle\psi^*|R_2\rangle \neq 0 \text{ (although much smaller than 1)}$$

and therefore R'_1 and ψ and $R'_2 = \psi^*$. The opposite relations are true in the product channel. The electronic coupling therefore vanishes on the asymptotes. In practice ψ and ψ^* are defined by truncated CIs restricted to a subspace S of determinants, defining a projector P

$$P = \sum_{I\in S}|\Phi_I\rangle\langle\Phi_I|$$

$$(PHP)\psi = E\psi$$

$$(PHP)\psi^* = E^*\psi^*$$

$$\psi = \sum_{I\in S} C_I\Phi_I \qquad \psi^* = \sum_{I\in S} C_I^*\Phi_I$$

The above procedure of projection plus orthogonalization is used, and one obtains two orthogonal nearly diabatic zeroth-order wave functions R'_1 and R'_2. Now $\langle R'_1|\mathcal{H}|R'_1\rangle$, $\langle R'_2|\mathcal{H}|R'_2\rangle$, and $\langle R'_1|\mathcal{H}|R'_2\rangle$ represent zeroth-order diabatic energies and coupling. The effect of the configurations outside S may be easily included to the second order[12] in a quasi degenerate perturbative approach[13]

$$\langle R'_i|\mathcal{H}^{\text{eff}}|R'_j\rangle = \langle R'_i|\mathcal{H}|R'_j\rangle + \sum_{K\notin S}\frac{\langle R'_i|\mathcal{H}|\Phi_k\rangle\langle\Phi_k|\mathcal{H}|R'_j\rangle}{E_j^0 - E_k^0}$$

where E_j^0 and E_k^0 are the zeroth-order energies of R'_j and Φ_k. In principle this effective Hamiltonian would be nonhermitian since E_1^0 may be different from E_2^0, but, as will be seen later, the diabatic potential surfaces are close in energy and a mean value E_0 has been taken, insuring the hermiticity.

The diagonalization of the second-order corrected 2 × 2 effective Hamiltonian must give us a second-order corrected estimate of the adiabatic potential surfaces. Of course the subspace S initially selected for the zeroth-order representation of ψ and ψ^* must be of equal quality for the whole potential surface, i.e., defined as the union of all the determinants which appear as important (coefficient larger than a given threshold) in one geometry at least. In practice when the size of that union is limited to 200 determinants, the quality of the zeroth-order wave functions is moderate, some of the selected determinants being of negligible importance for the considered geometry. The perturbation process cannot completely compensate that lack of precision and the surface does not match perfectly the independently calculated asymptotes or transition complex. These discrepancies, which will appear by comparing the adiabatic surfaces with the values given on Tables II and III give a measure of the uncertainty of the perturbative calculation of the effective Hamiltonian.

(C) **Direct Valence Bond Calculations.** Some direct valence bond (VB) calculations have also been performed, for the sake

(8) Barthelat, J. C.; Durand, Ph. *J. Chim. Phys.* **1974**, 7–8, 1005.
(9) Huron, B.; Malrieu, J. P.; Rancurel, P. *J. Chem. Phys.* **1973**, *58*, 5745. Daudey, J. P.; Malrieu, J. P. In *Current Aspects of Quantum Chemistry*; Elsevier Science Publishing Co.: Amsterdam, 1982; p 35. Evangelisti, S.; Daudey, J. P.; Malrieu, J. P. *Chem. Phys.* **1983**, *75*, 91.
(10) Möller, C.; Plesset, M. S. *Phys. Rev.* **1934**, *46*, 618.
(11) Cederbaum, L. S.; Köppel, H.; Domcke, W. *Int. J. Quant. Chem. Symp.* **1981**, *15*, 251.
(12) Cimiraglia, R.; Malrieu, J. P.; Persico, M.; Spiegelmann, F. *J. Phys. B* **1985**, *18*, 3073.
(13) van Vleck, J. H. *Phys. Rev.* **1929**, *33*, 467. Bloch, C. *Nucl. Phys.* **1958**, *6*, 329. Shavitt, I.; Redmon, L. T. *J. Chem. Phys.* **1980**, *73*, 5711.

Table I. Atomic Electroaffinities (in eV)

	H	Li	Cl
calcd	0.65	0.57	3.01
exptl	0.72[a]	0.62[b]	3.63[a]

[a] Hotop, H.; Lineberger, W. C. *J. Phys. Chem.* **1985**, *14*, 731. [b] Stwalley, W. C.; Koch, M. E. *Opt. Eng.* **1980**, *19*, 71.

of comparison with the diabatic approach presented above. The valence bond (VB) computational method that we have used has been fully described elsewhere and tested for its reliability[14] and will only be briefly summarized here. The basic feature of that method is that it deals with atomic orbitals (AOs) which are strictly localized on a single atom, with no delocalization tail of any kind on another atom. This way the correspondence between a bonding scheme and the valence bond functions (VBFs) is fully ensured. These VBFs are nothing but the analogues of configurations in MO-CI theory, with the difference being that the VBFs are not orthogonal to each other. The energies of the various states, diabatic or adiabatic, are computed by nonorthogonal CI among the VBFs.

The AOs are determined through separate Hartree–Fock calculations on the neutral isolated atoms in their ground states. This provides two kinds of AOs: the virtual ones and the occupied ones, hereafter called SCF-optimized orbitals.

Each relevant bonding scheme is associated with a VBF having the corresponding orbital occupancy and spin coupling. These VBFs are constructed with SCF-optimized AOs and are called "elementary VBFs". To ensure an optimal description of each bonding scheme, we add in the CI some complementary VBFs which are systematically generated from the elementary VBFs by monoexcitations from an SCF-optimized AO to a virtual AO centered on the same atom. In addition to these monoexcitations, two kinds of diexcitations are also included in the CI: (i) all the intraatomic excitations among the AOs of the X-fragment, to take the radial correlation of the corresponding electron pair into account, and (ii) some diexcitations corresponding to two simultaneous monoexcitations on different atoms in the same elementary VBF. Such diexcitations are added only if the product of the coefficients of the two corresponding monoexcitations is larger than a given threshold T. In this study, T has been fixed to 0.01.

The two main Lewis structures that are required to describe a reaction of the type $A^- + BC \rightarrow AB + C^-$ are **1** and **2**, in which the bond between two atoms is understood as an optimized mixture

$$\underset{\mathbf{1}}{A^-\ B\text{–}C} \qquad \underset{\mathbf{2}}{A\text{–}\ B\ C^-}$$

of its covalent and ionic components. In accord, the elementary VBFs used to describe, e.g., structure **1** include those displaying a covalent σ bond between B and C, but also the ionic components of the type $A^-B^+C^-$ and $A^-B^-C^+$, and lastly the π-type structures, in which the p orbitals of the B and C centers, perpendicular to the axis, are spin-coupled. Similar VBFs are generated for the description of **2**. A third Lewis structure, **3**, can formally be generated and has therefore been included.

$$\underset{\mathbf{3}}{A^\bullet\ B^-\ C^\bullet}$$

As for the adiabatic states, they are simply obtained by CI among the complete set of VBFs that have been generated for structures **1**, **2**, and **3**.

III. Results

(A) Atomic, Diatomic, and Transition Complex Properties. The electroaffinities of the reacting atoms play a crucial role in Shaik and Pross's model and must be considered first. Table I gives the calculated and experimental values. One may notice that the basis set limitation results in significant underestimations of the electroaffinities.

Table II. Molecular Characteristics of the Diatoms (Neutral and Anionic)[b]

	neutral		anionic		molec electroaff (eV)	
	r_e (au)	D_e (eV)	r_e (au)	D_e (eV)	vertical	adiabatic
Li_2	5.15 (5.05)[a]	0.954 (1.06)[a]	5.85	0.83	–0.819	0.448 (0.45)[a]
LiH	3.086 (3.016)[a]	2.236 (2.515)[a]	3.26	1.88	0.28	0.30
Cl_2	3.854 (3.758)[a]	1.529 (2.504)[a]	5.006	1.058 (1.26)[a]	<1.	2.540 (2.39)[a]

[a] Huber, K. P.; Herzberg, G. *Constants of Diatomic Molecules*; Van Nostrand Reinhold: New York 1979. [b] Values between parentheses are experimental ones.

Table III. $A^- + BB \rightarrow (ABB)^-$ Process; Adiabatic Energy Difference between the Two Entrance Channels and Characteristics of the Transition Complex[c]

		(ABB)⁻ complex characteristics		
	EA(A) – EA(BB)	r_{AB} (au)	R_{BB} (au)	stability/ (A^- + BB) (eV)
$Li^- + Li_2$	0.12 (0.37)	5.76	i.d.	0.97
$H^- + Li_2$	0.20 (0.27)	3.26	6.25	2.46
$Cl^- + Cl_2$	0.52 (1.24)	4.45 (4.22)[a]	i.d.	0.93 (0.65)[b]

[a] Bogaard, M. P.; Peterson, J.; Rae, A. D. *Acta Crystallogr. Sect. B* **1981**, *37*, 1357; in solid phase. [b] Reference 18. [c] Experimental information parentheses.

The diatomic characteristics are given in Table II. The main error concerns the underestimation of the bonding energy of Cl_2 (by 0.97 eV out of 2.5 eV), a well-known problem for halogens, which can only be solved by the use of large basis sets and extensive CI. The error is much smaller on Cl_2^-, which has a longer bond, and the molecular electroaffinity is finally overestimated.

The differences between the electroaffinities of A and BB for the $A^- + BB \rightarrow AB + B^-$ reaction, which is the main variable of the Shaik and Pross's model, are reported in Table III. The errors on these differences are very large, especially for $Cl^- + Cl_2$ where the two errors add; this is the reason why a shift of the asymptotes of the diabatic surfaces will be attempted for that reaction.

The $(ABB)^-$ complex geometry has been optimized at the CI level, and the results also appear in Table III. In these three problems, the complex is stable with respect to the entrance A^- + BB and product AB + B^- channels. Spectroscopic information is available on Cl_3^-; the calculation overestimates slightly the Cl–Cl bond lengths, our value being equal to that proposed by recent MRDCI calculations of Peyerimhoff[15] and Alvarez.[16]

(B) The $Li^- + Li_2$ Reaction. For symmetrical reactions (A^- + BA → AB + A^-), the two diabatic potential surfaces are symmetrical with respect to the plane $r_{AB} = r_{BC}$. They intersect in that plane. One of them is drawn in Figure 2; it presents two orthogonal talwegs, with a very regular shape. The entrance valley presents a minimum ($r_{bc} \simeq 9$ Bohr, $r_{ab} \simeq 5.5$ Bohr), which can be understood as due to the polarization of Li_2 by Li^- since delocalization between Li_2 and Li^- is forbidden. The point of minimum energy on the crossing seam corresponds to $r_{AB} = r_{BC} = 5.76$ Bohr, at an energy ~4.2 kcal/mol below the entrance ground-state channel.

The (r_{AB}, r_{BC}) dependence of the electronic coupling h_{12} is given in Figure 3. It presents a maximum amplitude for $r_{AB} = r_{BC} = 6.3$ Bohr, but, in that region, h_{12} is weakly dependent on $r_{AB} + r_{BC}$ for $r_{AB} = r_{BC}$. As a result the minimum of the adiabatic potential surface is very close to the minimum of the crossing seam

(14) Maître, P.; Lefour, J. M.; Ohanessian, G.; Hiberty, P. C. *J. Phys. Chem.* **1990**, *94*, 4082.

(15) Sannigrahi, A. B.; Peyerimhoff, S. D. *Chem. Phys. Lett.* **1987**, *141*, 49.

(16) Novoa, J. J.; Mota, F.; Alvarez, S. *J. Phys. Chem.* **1988**, *92*, 6561.

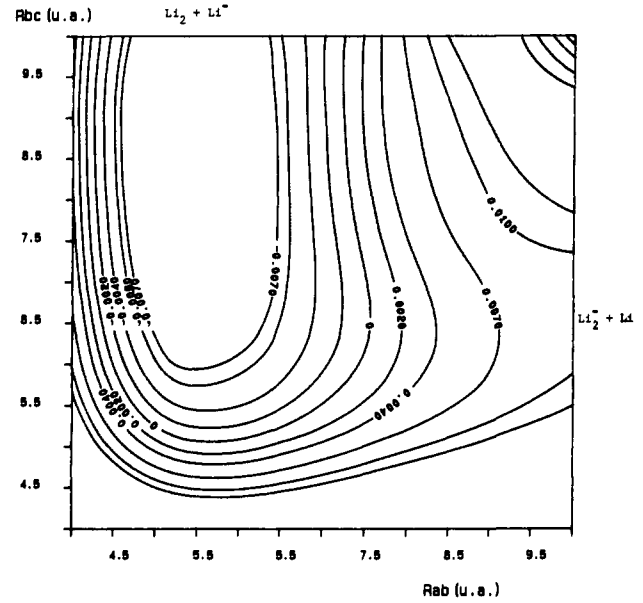

Figure 2. Diabatic potential energy surface for the Li_3^- system, connecting the $Li^- + Li_2$ entrance channel to the $Li_2^- + Li$ product channel. Energies are in au, the zero of energy being in the entrance channel.

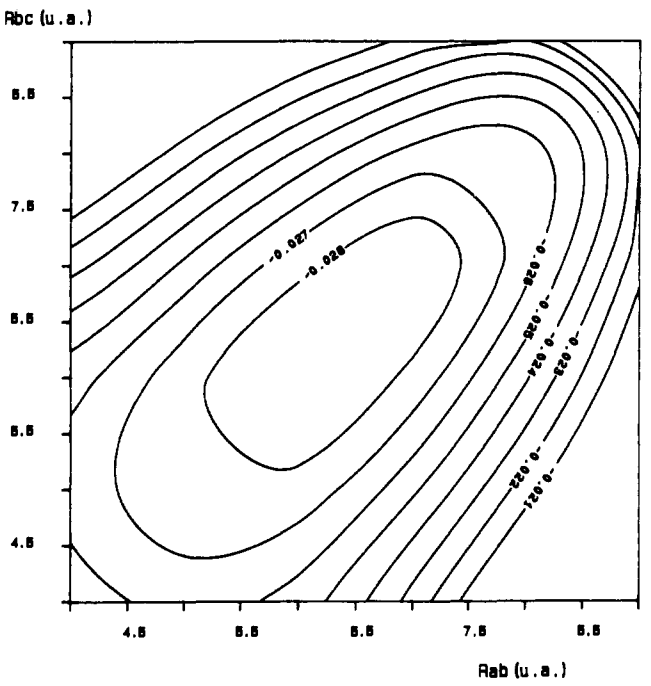

Figure 3. Electronic coupling between the two diabatic states of the Li_3^- problem (in au).

($r_{AB} = r_{BC} = 5.76$ Bohr). At this distance $h_{12} = 18.1$ kcal/mol, so that the minimum of the adiabatic potential surface is 22.3 kcal/mol below the entrance channel. Figure 4a,b gives the $^1\Sigma^+$ ground and excited adiabatic potential surfaces; the excited potential surface presents a barrier with a saddle point close to the minimum of the crossing seam.

In view of the simplicity and regularity of the diabatic potential curve it is tempting to fit the numerical values by a simple analytic formula, and the LEPS form[7] seems a natural choice.

The adequacy of such an analytical form appears from Figure 5 which compares the spline interpolation of the numerical grid with the optimized LEPS potential in the crucial region of interaction.

(C) The Cl^- + Cl_2 Reaction. Due to the large number of electrons and the size of the basis set, the computation requires 21 h on a Microvax 2 for each conformation, and only 30 points have been calculated, essentially around the reaction path. The

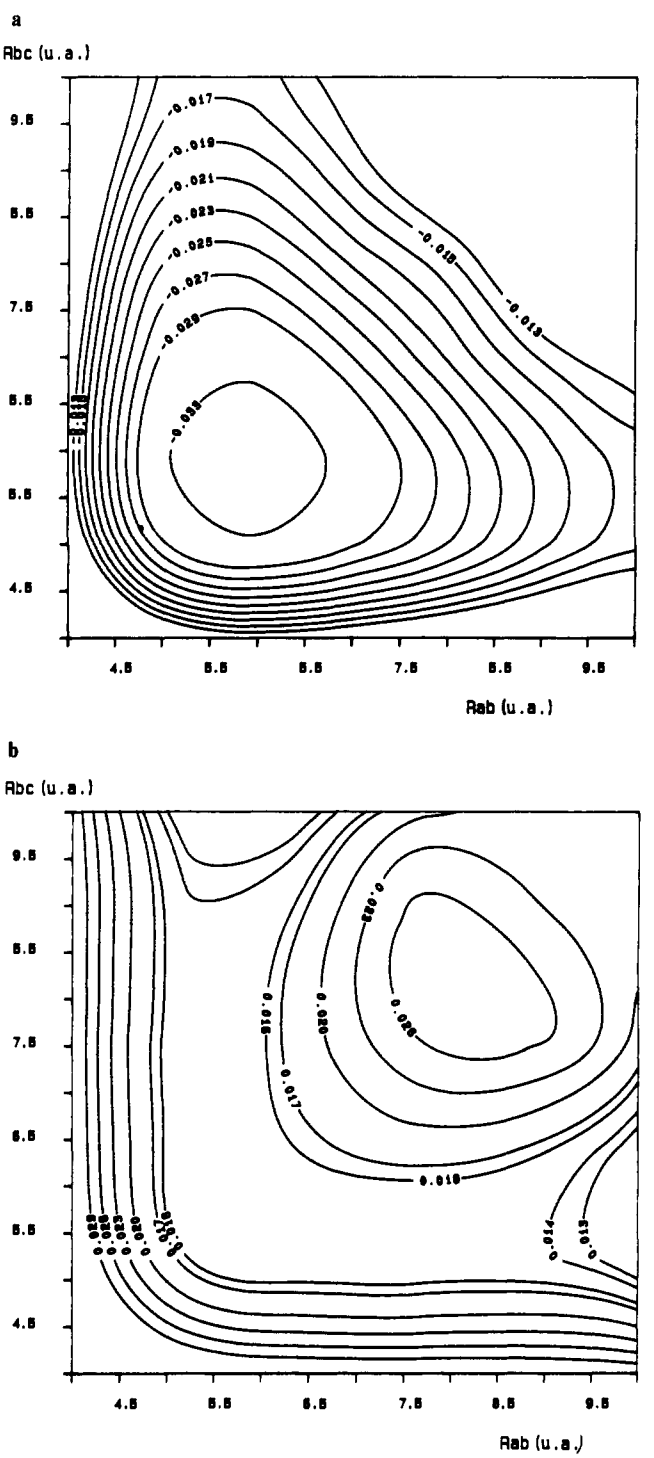

Figure 4. (a) $^1\Sigma^+$ ground state adiabatic potential energy surface for the Li_3^- problem (in au). The zero of energy is the entrance channel $Li^- + Li_2$. (b) $^1\Sigma^+$ excited state adiabatic potential energy surface.

LEPS function for the diabatic surface has been fitted on these points. The minimum of the crossing seam of the two surfaces is obtained for $r_{AB} = r_{BC} = 4.45$ Bohr, close to the Cl_3^- experimental geometry (cf. Table III).

In view of the poor quality of the calculated Cl_2 (and to a lesser extent Cl_2^-) potential curves, we have decided to recalculate a LEPS function which keeps its interaction term to its previously fitted values and to introduce the correct spectroscopic values of Cl_2 and Cl_2^- on the asymptotic part of the LEPS function. Such a procedure is expected to give improved diabatic potential curves.

Regarding the electronic coupling between the two diabatic surfaces, one may notice that for $r_1 = r_2$ its value is equal to one-half of the energy difference between the ground $^1\Sigma_g^+$ state

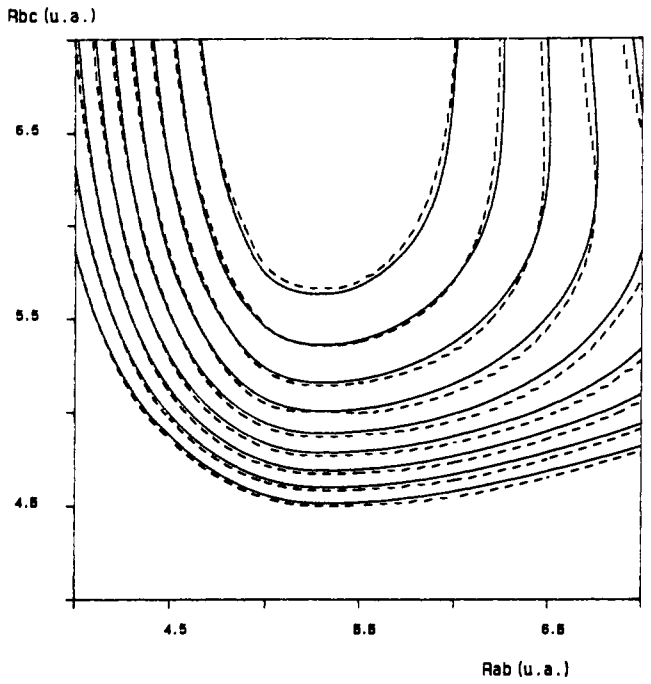

Figure 5. Comparison between the calculated (full lines) and LEPS (dotted lines) diabatic potential energy surface for the Li_3^- problem. The isoenergy curves vary from −0.008 to +0.008 au with a 0.003 au step.

and the lowest $^1\Sigma_u^+$ excited state. For Cl_3^- this quantity is known to be equal to ~5.10 eV from experiment,[17] while our estimate was 6.27 eV. We have therefore reduced the amplitude of the electronic coupling by a constant factor (5.1/6.27) and recalculated the adiabatic energies. The empirically corrected energy of the Cl_3^- complex, is finally predicted to be 0.63 eV more stable than $Cl_2 + Cl^-$, in good agreement with the experimental estimate (0.65 eV from ref 18 and the experimental D_e of Cl_2).

(D) The $H^- + Li_2$ Reaction. For that unsymmetrical reaction, the diabatic potential energy surfaces are different. They are given in Figure 6a,b. The $H^- + Li_2 \rightarrow HLi^-$ Li surface (i.e., the one which corresponds to the entrance channel) presents again two orthogonal talwegs, with a minimum for a compact geometry $r_{HLi} \simeq r^e_{HLi}$, $r_{Li_2} \simeq r^e_{Li_2}$. This minimum is 1.7 eV below the entrance channel, and it may be viewed as an $H^-(Li_2)$ complex without electronic delocalization but a strong polarization of the Li_2 molecule.

The second diabatic potential surface ($HLi + Li^- \leftrightarrow H + Li_2^-$), i.e., the one coming from the ground-state product, presents no minimum. The crossing seam is displaced toward the product channel. Its minimum takes place near $r_{HLi} = 3.2$ Bohr and $r_{LiLi} \simeq 7.1$ Bohr.

The electronic coupling presents a regular shape (cf. Figure 7), with a maximum amplitude (~1 eV) for $r_{HLi} \simeq 4.6$ Bohr, $r_{LiLi} \simeq 7.3$ Bohr. The effect of the interaction between the diabatic states is to create an overall minimum in the lowest adiabatic state at longer interatomic distances than those of the entrance diabatic surface minimum. The equilibrium distances are $r_{HLi} \simeq 3.26$ and $r_{LiLi} \simeq 6.25$ Bohr. The adiabatic ground and excited states of $^1\Sigma^+$ symmetry appear in Figure 8 (parts a and b, respectively). The first one presents a simple well between two valleys, whereas the second one exhibits a saddle point in the entrance channel.

(E) The $Cl^- + CH_3Cl$ Reaction. The same procedure has been applied to a more chemical problem, namely the $Cl^- + CH_3Cl$ S_N2 reaction. The adiabatic reaction path in the gas phase has been the subject of a large number of theoretical works, which are referenced in three recent papers including electronic correlation effects through either MP2[18,19] or single and double CI.[20]

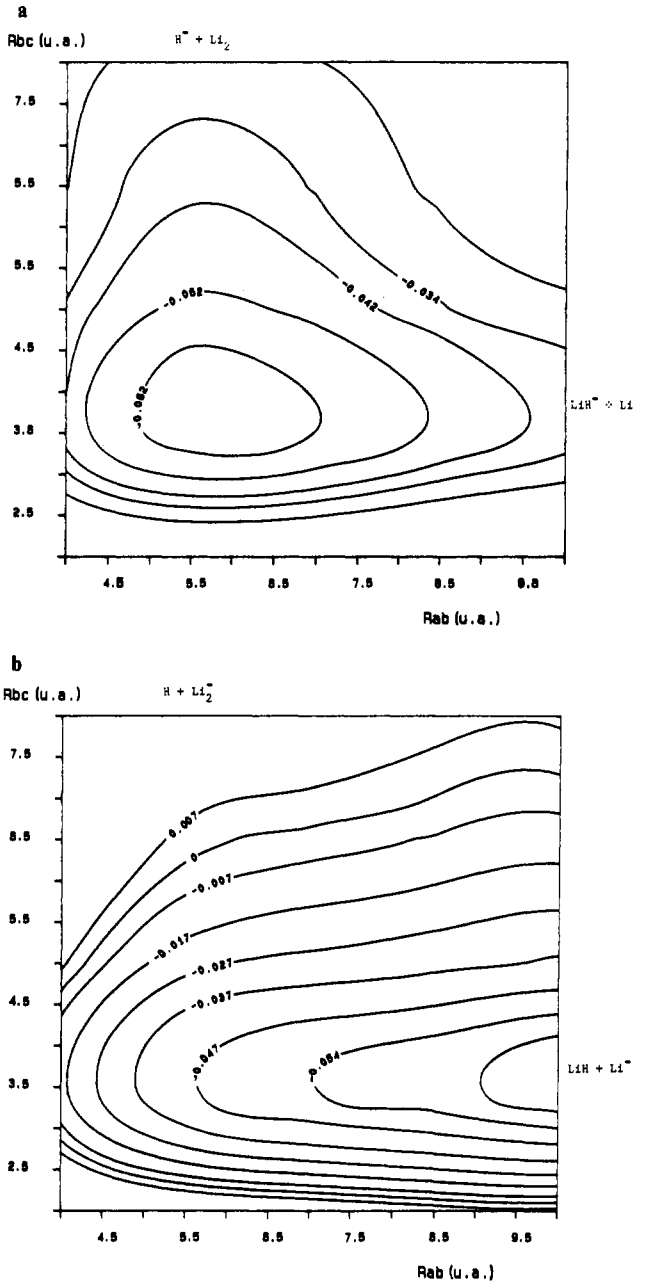

Figure 6. (a) Diabatic PES for the Li_2H^- problem, connecting the H^- + Li_2 entrance channel (taken as the zero of energy) to the HLi^- + Li excited product channel. Energies are in au. (b) Diabatic PES for the Li_2H^- problem, connecting the excited H + Li_2^- entrance channel to the HLi + Li^- ground-state product channel. Same zero of energy as in Figure 6a.

The geometries of the reactants and of the complex optimized in the latter work have been used hereafter together with a double-ζ + polarization basis set the vertical entrance gap (energy difference between Cl^-/CH_3Cl and Cl/CH_3Cl^-) is calculated to be 137 kcal/mol at the HF level and 144 kcal/mol at the CI (multireference MP2) level. The symmetrical transition complex is calculated to lie at 4.1 kcal/mol above the entrance channel at the SCF level; this barrier height increases slightly under the inclusion of correlation since our CIPSI value is 6.4 kcal/mol. The result compares quite well with the SDCI estimate[20] (7.3 kcal/mol) and is a little larger than the MP2 values (4.5 kcal/

(17) Robin, B. M. *J. Chem. Phys.* **1964**, *40*, 3369.
(18) Shi, Z.; Boyd, R. J. *J. Am. Chem. Soc.* **1989**, *111*, 1575.
(19) Tucker, S. C.; Truhlar, D. G. *J. Phys. CHem.* **1989**, *93*, 8138.
(20) Vetter, R.; Zülicke, L. *J. Am. Chem. Soc.* **1990**, *112*, 5136.
(21) Robbiani, R.; Francklin, J. R. *J. Am. Chem. Soc.* **1979**, *101*, 764.
(22) Kabbaj, O. K.; Volatron, F.; Malrieu, J. P. *Chem. Phys. Lett.* **1988**, *147*, 353.
(23) Keil, F.; Ahlrichs, R. *J. Am. Chem. Soc.* **1976**, *98*, 4787.

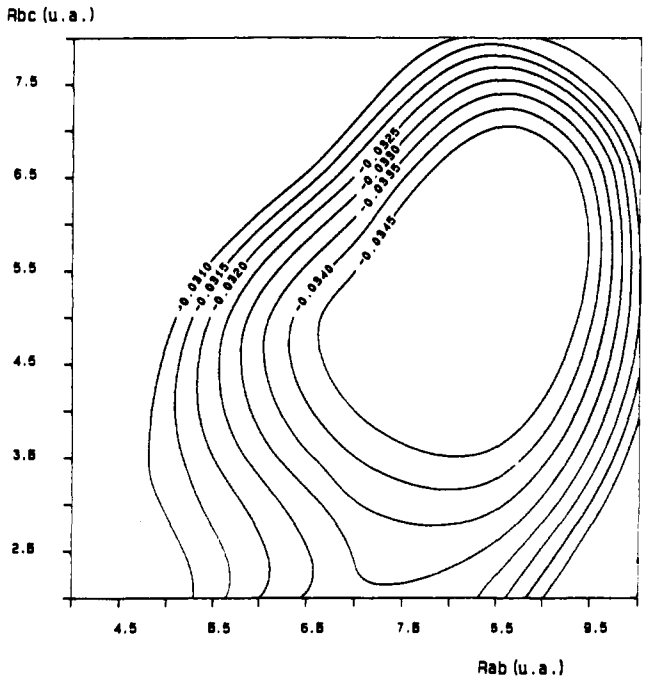

Figure 7. Electronic coupling between the two diabatic states of the HLi_2^- problem.

Table IV. Main Features of the Energy Profiles (in kcal·mol^{-1})[a]

	Li_3^-	Cl_3^-	Li_2H^- vs entrance channel	Li_2H^- vs product channel
entrance gap (G)				
vert	5.1	49.6	3.12	8.01
adiab	3.7	12.0 (28.6)	1.84	0.67
height of the crossing point (fG)	−4.2	41.7 (44.4)	−36.63	−5.24
amplitude of the electronic interaction at the crossing point (B)	18.1	72.3 (59.0)	21.76	
stabilization energy of the complex (E_S)	22.3	21.4 (14.6)	56.78	25.39

[a] For Cl_3^- the values in parentheses are obtained from rescaling of the asymptote and coupling term on experimental data.

mol[19]). For this geometry the diabatic potential surfaces cross at an energy which is 50 kcal/mol above the entrance channel. The interaction B between the two diabatic configurations is 50 kcal/mol at the SCF level and 56 kcal/mol after the variational + perturbational treatment. This quantity is somewhat larger than usually expected.

IV. Correlation Diagrams and Discussion

A convenient way to get closer to the VB correlation diagrams consists in focusing on the ground-state adiabatic reaction pathway. The information is then reduced to diabatic and adiabatic profiles and to the variation of the electronic coupling. For convenience we have defined a degree of advancement of the reaction by the index

$$\rho = \left(1 - \frac{r_e(AB)}{r(AB)} + \frac{r_e(BC)}{r(BC)}\right) \Big/ 2$$

which varies from 0 (entrance channel) to 1 (product channel), the crossing and transition complex appearing at $\rho = 1/2$ for symmetrical reactions.

The shapes of the diabatic and adiabatic potential curves along the reaction path appear in Figures 9–11 for the three reactions.

These profiles may be directly related to the Shaik's VB diagrams, of which they might be considered as a quantitative transcription. The relevant parameters G (entrace gap), fG (height of the crossing point), B (electronic coupling), E_s (energy stabilization of the complex with respect to the entrance channel) are summarized in Table IV. These results deserve the following comments.

(i) In Figures 9–11 the upper state of the entrance channel is the *vertical* charge-transfer state. It would be meaningless to draw an upper diabatic profile which does not correspond to the same pathway as for the ground state. Therefore the connection between the gap G in the entrance channel and the experimental difference of electroaffinities EA(A) − EA(BC) is quite arbitrary; the experimental molecular electroaffinities are adiabatic (i.e., involving a relaxed geometry for BC^-), and the vertical and adiabatic electroaffinities may be very different as mentioned in the figures. For Li_2 (see Table II) the difference between EA^{vert} and EA^{adb}

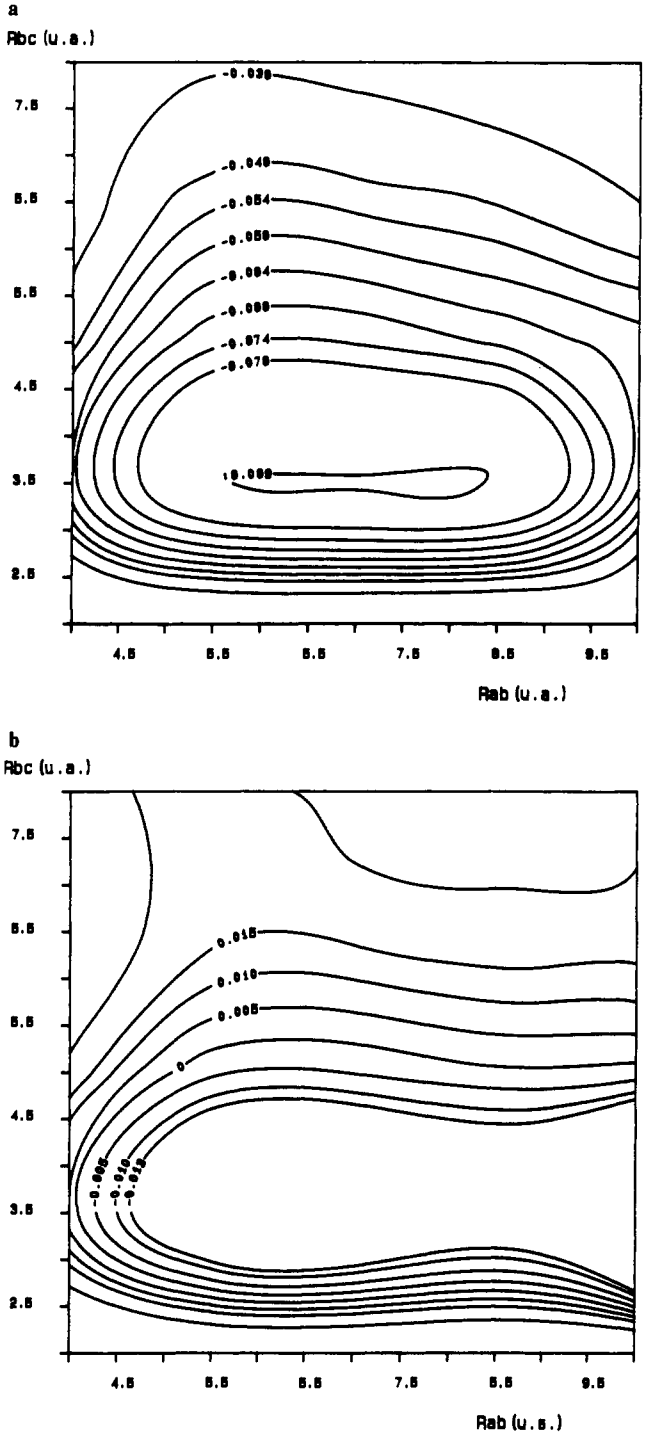

Figure 8. (a) Ground-state adiabatic PES for Li_2H^-. The energies are in au, the zero being taken from the $Li_2 + H^-$ entrance asymptote. (b) Lowest $^1\Sigma^+$ excited state adiabatic PES for Li_2H^- (energies in au).

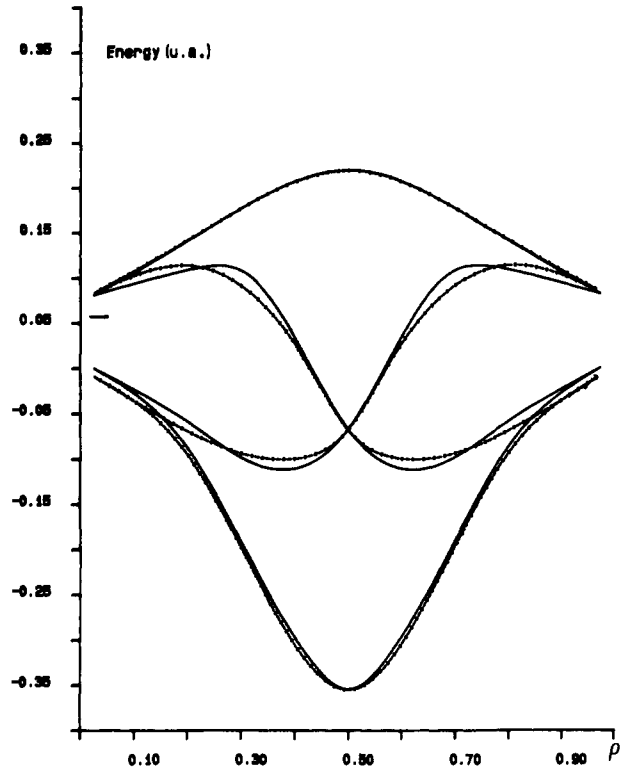

Figure 9. Diabatic (middle curves) and adiabatic (upper and lower curves) energy profiles along the reaction pathway for Li_3^-: full lines, calculated profiles; dotted lines, values obtained from a LEPS function. The straight lines in the entrance channel indicate the lowest point of the excited entrance channel, i.e., the adiabatic gap.

is larger than EA^{adb}, Li_2^- being unbound at $r = r_{BC}$ (Li_2). The vertical EA of Cl_2 is certainly smaller than the adiabatic one by more than 1 eV. This is a serious question addressed to the empirical evaluations of Shaik's gap G from the experimental electroaffinities, at least for small systems. Notice however that for organic molecules the variation of the electroaffinity under the relaxation of the anion is certainly weaker.

(ii) The lowest point of the crossing seam actually corresponds to the transition complex geometry for the studied symmetrical reaction, due to the weak variation of the electronic coupling under the variation of $r_{AB} + r_{BC}$ in that region. For HLi_2^- the crossing does not occur at the stable geometry of the complex but further in the product channel. It would be interesting to study a nonsymmetrical problem presenting a barrier, in order to see whether the crossing point and the saddle point have close enough geometries.

(iii) The electronic coupling, which presents a maximum amplitude in the crossing region, varies significantly from one system to another; we find 18.1 kcal/mol for Li_3^- and 22 kcal/mol for Li_2H^-, and the experiment gives 57 kcal/mol for Cl_3^-. The same value is obtained for $ClCH_3Cl^-$. For H_3^- we had obtained 28 kcal/mol.[19]

(iv) For nonsymmetrical reactions, it seems more natural to treat the entrance and product channels on an equal foot.

V. Comparison of Diabatic MO-CI Calculations with Direct Valence Bond Calculations

We have performed some calculations of curve crossing diagrams by means of the direct VB method, for the sake of comparison with the diabatic MO-CI approach presented above, as applied to the reactions $Li^- + Li_2$ (this work) and $H^- + H_2$ (ref 19).

(A) Adiabatic Energy Profiles. The ground states of the H_3^- and Li_3^- clusters have been calculated by nonorthogonal CIs of dimensions 225 and 268, respectively, and the same CI space has been kept for reactants, cluster, and products in each reaction.

The potential well obtained for the Li_3^- cluster, relative to $Li^- + Li_2$, amounts to 19.5 kcal/mol, in good agreement with the value of 22.3 computed in the MO-CI formalism, if one considers the small dimension of the VB CI. It should be noted that the reaction is quite well-described by an interplay of structures **1** and **2** only, as the stabilizing effect of structure **3** only amounts to 1.5 kcal/mol in the cluster geometry and does not contribute to the ground states of reactants and products.

The barrier for the reaction $H^- + H_2$ is also reasonable, 13.97 kcal/mol as compared to the MO-CI value 10.6 kcal/mol, and structure **3** is now found to play a nonnegligible role, stabilizing the transition state by 8.5 kcal/mol.

(B) Diabatic Curves. Some diabatic curves analogous to those displayed in Figure 9 can be directly computed by the VB method and are obtained as follows.

As the ground state of the reactants is exclusively composed of structure **1** whereas the excited product is a mixture of **1** and **3**, the diabatic curve connecting those two states is a variational mixture of the VBFs of **1** and **3**. Similarly, the other diabatic curve is a mixture of **2** and **3**. Only the points corresponding to the reactants, cluster, and products geometries have been calculated, as this is sufficient to get the crucial parameters of the VB diagrams: f, B, and G.

For $Li^- + Li_2$, the two diabatic curves cross 4.9 kcal below the ground state of the reactants, yielding the value 14.6 kcal/mol for the avoided crossing interaction (the B factor). The diabatic crossing point is, on the other hand, 39.3 kcal/mol above the reactants ground state for the reaction $H^- + H_2$, with a B factor of 25.3 kcal/mol. All these values match very well with those

Table V. Critical Parameters of Shaik and Pross Curve Crossing Diagrams, as Calculated with the Direct Valence Bond and MO-CI Techniques, for the Reactions $Li^- + Li_2$ and $H^- + H_2$[f]

	Li_3^-, VB	Li_3^-, MO-CI	H_3^-, VB	H_3^-, MO-CI
E_s[a]	−19.5	−22.3	13.97	10.6
B[b]	14.6	18.1	25.3	28.4
fG[c]	−4.9	−4.2	39.3	39.0
G[d]	10.2	5.1	59.5	56.8
G'[e]	13.7		124.6	

[a] Stabilization energy of the X_3^- complex, relative to $X^- + X_2$. [b] Amplitude of the electronic interaction at the crossing point. [c] Height of the crossing point, relative to $X^- + X_2$. [d] Vertical energy gap for the transfer $X^- + X_2 \rightarrow X^\bullet + X_2^-$, in the reactants' geometry, computed in the complete basis set. [e] Same as footnote *d*, but X_2^- is calculated without diffuse orbitals. [f] All energies are in kcal/mol^{-1}.

Table VI. Gaussian (3s,2p) Atomic Basis Set for H and (3s,2p,1d) for Li and Cl

atomic	shell type	exponent	contraction coefficient
H	s	13.2479	0.019293
		2.00313	0.133465
		0.455867	0.473667
		0.124695	1.0
		0.03	1.0
	p	1.12	1.0
		0.2	1.0
Li	s	2.464158	−0.110433
		1.991405	0.241067
		0.581880	0.889523
		0.070935	0.579231
		0.027095	0.461114
		0.007445	1.0
	p	0.10	1.0
		0.027	1.0
	d	0.12	1.0
Cl	s	7.577375	0.048867
		2.456871	−0.336200
		0.515165	0.624733
		0.188619	1.0
		0.058263	1.0
	p	2.179918	−0.138721
		1.288347	0.257682
		0.418131	0.525337
		0.137427	1.0
	d	0.65	1.0

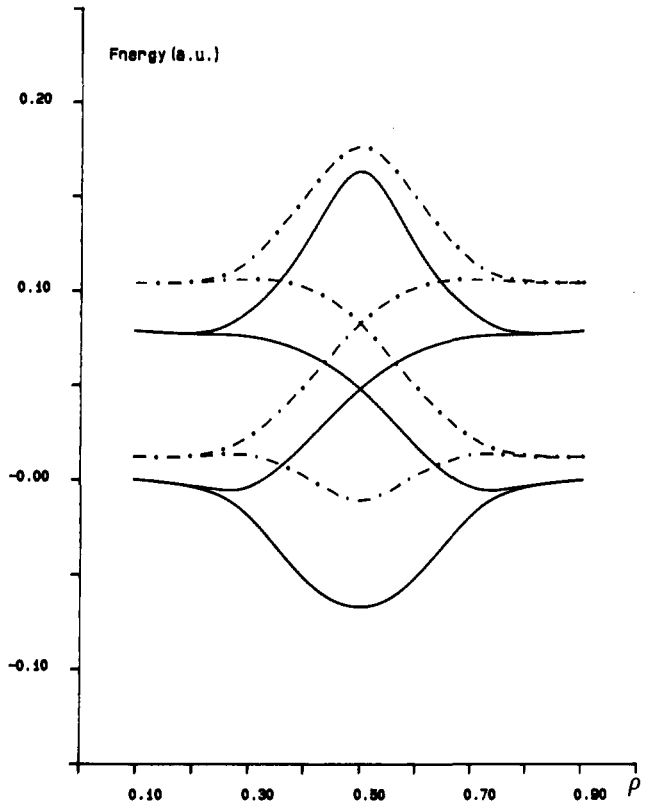

Figure 10. Same comment as for Figure 9, concerning Cl_3^-. The dotted lines here refer to profiles rescaled on experimental data.

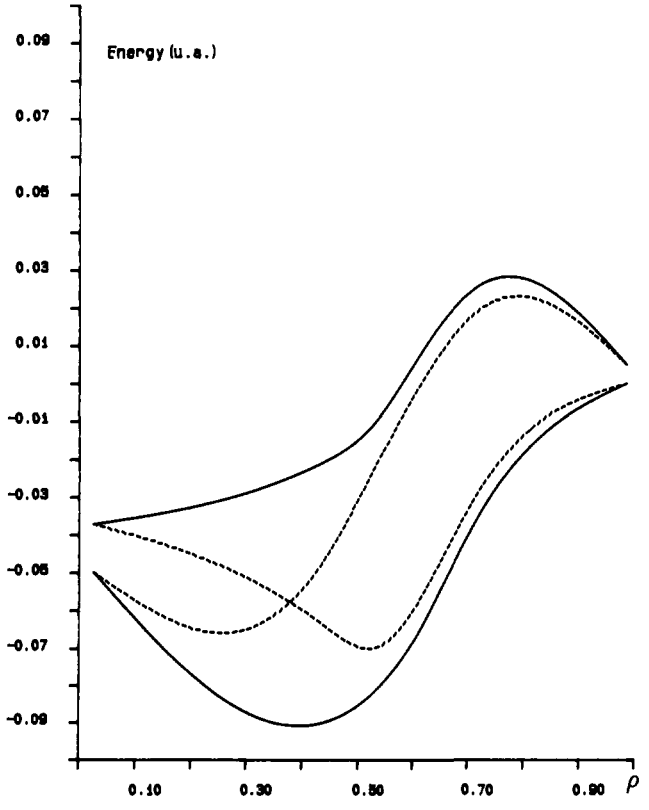

Figure 11. Same comment as for Figure 9, concerning Li_2H^-.

arising from the MO-CI diabatization technique, as shown in Table V.

(C) The *G* Factor. The vertical excitation energies, corresponding to the transition $X^- + X_2 \rightarrow X^\bullet + X_2^-$ in reactants geometry, reasonably agree with the results of MO-CI calculations (see Table V). However the unpaired electron in the X_2^- species is located in a diffuse orbital, and it may be argued that such a state does not really fit in the original VB diagrams is introduced by Shaik and Pross, for two reasons: (i) In many cases X_2^- is unstable with respect to the loss of one electron, so that its energy is extremely basis set dependent which does not make much sense since an optimization of the diffuse orbital would lead to an infinitely small exponent. (ii) In the original qualtitative diagrams,[3,4] a vertical excited state is referred to as "image of the products in the reactants geometry" (or vice versa). In such a state, the unpaired electron is located in a σ^* orbital, of valence nature.

It thus appears that the vertical excited state most faithful to the model is best calculated in a basis set devoid of diffuse orbitals. As an important extra advantage, this ensures that the diabatic curves remain monotonous from the crossing point to the excited state, instead of displaying a bump as in Figure 9, a sine qua non condition for the discussion on their curvatures to be relevant. Thus, the diffuse character of a diabatic curve, which naturally diminishes from the ground $(X^- + X_2)$ state to the crossing point, is prevented to mix with an intruder infinitely diffuse state as one approaches the excited charge-transfer state $(X^\bullet + X_2^-)$. Of course the lack of diffuse orbitals in the calculation of X_2^- leads to rather large values of G (labeled G' in Table V, entry 5), especially for the reaction $H^- + H_2$, which in return yields the value 0.32 for the curvature factor f. Let us not that this latter value agrees very well with the expectations of Shaik and Pross for the S_N2 reactions, for which the $H^- + H_2$ reaction has sometimes been taken as a model.[3,20]

It should be noted that for qualitative applications of the diagrams, the G factor can very well be estimated at the Hartree–Fock level. Indeed, the large error on the ionization potential of X^-, due to lack of electron correlation, is compensated by a similar error on the electron affinity of X_2. The Hartree–Fock values of G, as calculated without diffuse orbitals in the X_2^- species, are somewhat smaller (respectively 1.4 and 99.3 kcal/mol for X = Li, H) than the VB values, because the lack of left–right electron correlation affects X_2 more than X_2^-, but the error must be systematic, so that the Hartree–Fock and VB tendencies should be the same, which is all that matters.

VI. Conclusion

This paper shows that the qualitative VB correlation diagrams proposed by Shaik, which consider the allowed S_N2 reactions as two-state problems, may receive a quantitative transcription through MO-CI nearly diabatic approaches. Despite this basic confirmation, the results raise a series of questions regarding the assumptions of the VB model, which have been developed in the preceding section and which would deserve analysis through further examples for reactions presenting barriers. The method may be applied as well to more realistic systems.

The method in principle gives two eigenstates (of $^1\Sigma^+$ symmetry in colinear systems) and one might think to use the information (especially the analytic interpolations of the diabatic surfaces and electronic coupling) to calculate cross sections for processes with and without electron transfer, reactive or not. One should however keep in mind that intruder states of π symmetry may cross the upper $^1\Sigma^+$ surface and mix under the ABC bending mode. This is the case for Cl_3^- (see ref 13) and appears likely for Li_3^- where ΔE ($^1\Sigma_g^+ - {}^1\Sigma_u^+$) $\simeq$ 1.3 eV.

For the two sample reactions $H^- + H_2$ and $Li^- + Li_2$, the diabatic curves as generated by this method are similar in shape to those arising from direct VB calculations, as far as the crucial parameters of Shaik and Pross's diagrams are taken as a basis for comparison. For the G parameter, the use of a valence basis set, devoid of diffuse orbitals, may be advocated for the calculation of the charge-transfer state, as yielding diabatic curves most faithfully corresponding to the original model of curve crossing diagrams. That difficulty may also be solved rigorously in the MO-CI approach since diabatization techniques may be used to search the *valence* state of an unbound anion, which is embedded in a continuum. The method has been successfully applied to H_2^-[24]

(24) Komiha, N.; Daudey, J. P.; Malrieu, J. P. *J. Phys. B* **1987**, *20*, 4375.

and HCl^-,[25] but its introduction in the present problem would complexify the procedure since the diabatization would act on more than two eigenstates of the CI problem.

The use of diabatic descriptions may be especially tempting when basis set and CI limitations introduce serious deviations from experiment. Due to the expected constant physical content of the diabatic function, a proper fitting on the asymptotes becomes possible, which would be impossible in adiabatic approaches. This has been done frequently on diatomic problems. Here the diabatic surface matches two different (although related) asymptotes in the entrance and product channel, and a double fitting is necessary on both asymptotes. The LEPS fit of the diabatic surface is especially convenient to proceed to such adjustments on experiment.

Acknowledgment. Thanks are due to Dr. F. X. Gadêa for helpful discussions. One of us (O.K.K.) acknowledges the support of the Action Intêgrêe Franco-Marocaine.

Registry No. Li_2, 14452-59-6; Li^-, 14808-04-9; H^-, 12184-88-2; H, 12385-13-6; Li_2^-, 11062-41-2; Cl, 16887-00-6; Cl_2, 7782-50-5; CH_3Cl, 74-87-3.

(25) Rajzmann, M.; Spiegelmann, F.; Malrieu, J. P. *J. Chem. Phys.* **1988**, *89*, 433.

Reaction Path Study of Ligand Diffusion in Proteins: Application of the Self Penalty Walk (SPW) Method To Calculate Reaction Coordinates for the Motion of CO through Leghemoglobin

Wieslaw Nowak,[†] Ryszard Czerminski,[‡] and Ron Elber*

Contribution from the Department of Chemistry, M/C 111, University of Illinois at Chicago, P.O. Box 4348, Chicago, Illinois 60680. *Received December 7, 1990*

Abstract: Reaction coordinates for the diffusion of carbon monoxide through leghemoglobin are calculated by using the recently developed SPW algorithm (Self Penalty Walk).[1] The new algorithm makes it possible to study in a systematic way reaction coordinates in molecules with more than 1000 atoms. To explore properties of similar (but distinct) reaction coordinates, three diffusion paths were calculated. The separate coordinates were generated from different initial guesses for the paths, which were obtained from classical trajectories.[2] Analysis of the three calculated paths reveals that the "local" properties of the coordinates in the vicinity of the CO are very similar. The interaction energy profile of the carbon monoxide with the rest of the protein has a similar shape in the three paths, and the structural features of the local transition states are essentially the same. On the other hand, global protein properties vary considerably in the three paths. The macromolecule motions include many fluctuations that are not coupled to the diffusing ligand. It is concluded that while the density of alternative paths for the diffusion process may be very high, the close neighborhood of the ligand appears to be very much alike in the sampled paths. The diffusion process consists of two steps. In the first, the ligand hops from the heme pocket to another cavity in the protein matrix, and in the second it hops to the protein exterior. The first barrier is dominated by a tilt of a single residue (Phe 29 B9). The second barrier is more complex and includes many types of motions. In particular, global translations and rotations of helices C and G are involved.

I. Introduction

The reaction coordinate (RC) approach has been shown to be useful in the study of a variety of chemical processes of small molecules (<10 atoms).[3] The RC is helpful in estimating barrier heights for the reaction, in obtaining structural insight to the properties of the transition state, and finally, in quantitative calculations of the rate.

The RC is usually defined as the steepest descent path (SDP).[3] This definition guarantees a continuous description of the motion between the reactant and the product, with a low energy barrier.

Though successful for small molecules, tools for a few atoms are not necessarily adequate for studying RC in macromolecules (>1000 atoms). There are two serious difficulties in attempting to extrapolate from systems with several atoms to systems with thousands of atoms. The first obstacle is computational: It is far from easy to calculate reaction paths in large systems, and only recently appropriate tools were developed. Moreover, in large systems it is not clear if the concept of a *single* reaction coordinate is valid and if the SDP is the best description of the reaction coordinate.

Obviously in order to study properties of paths in macromolecules, one needs to calculate them first. We initiated a program to develop theoretical tools to study reaction paths in large molecular systems. These tools were tested on small molecules[1] (~20 atoms), and we apply them here to a macromolecule (1471 atoms). To the best of our knowledge, this is the first application of an automatic algorithm to calculate and compare different reaction coordinates in a system of comparable size. Here we address the problem of the diffusion of a small ligand through a protein matrix.

Diffusion of a small ligand from active sites buried in protein matrices attracted considerable theoretical and experimental attention over the years. Of special interest were the investigations of the diffusion of a small ligand (e.g., oxygen, carbon monoxide) in myoglobin, for which a wealth of data is currently available.[4]

Here we consider the diffusion in a "myoglobin variant"—lupine leghemoglobin. Leghemoglobin has the same evolutionary ancestor as myoglobin but binds oxygen significantly faster and more strongly.[5] Currently there is no clear structural or dynamical

[†] On leave from the Institute of Physics, N. Copernicus University, ul. Grudziadzka 5, PL-87-100 Torun, Poland.
[‡] Present address: Polygen, 200 Fifth Ave., Waltham, MA 02254.

(1) Czerminski, R.; Elber, R. *Int. J. Quantum Chem.* **1990**, *24*, 167.
(2) Czerminski, R.; Elber, R. *Proteins* **1991**, *10*, 70.
(3) For reviews, see for instance: Muller, K. *Angew. Chem., Int. Ed. Engl.* **1990**, *1*, 19. Bell, S.; Crighton, J. S. *J. Chem. Phys.* **1990**, *80*, 2464.
(4) For a recent review, see: Brunori, M.; Coletta, M.; Ascenzi, P.; Bolognesi, M. *J. Mol. Struct.* **1989**, *42*, 175.

0002-7863/91/1513-5627$02.50/0